Supporting Information

Metallic few-layered VSe_2 nanosheets: high two-dimensional conductivity for flexible in-plane solid-state supercapacitor

Chaolun Wang[a], Xing Wu[a, *], Yonghui Ma[b], Gang Mu[b], Yaoyi Li[c], Chen Luo[a], Hejun Xu[a], Yuanyuan Zhang[a], Jing Yang[a], Xiaodong Tang[a], Jian Zhang[a], Wenzhong Bao[d], Chungang Duan[a, e]

[a] *Key Laboratory of Polar Materials and Devices (MOE), Shanghai Key Laboratory of Multidimensional Information Processing, Department of Electronic Engineering, East China Normal University, 500 Dongchuan Road, Shanghai, 200241, China.*

[b] *State Key Laboratory of Functional Materials for Informatics, Shanghai Institute of Microsystem and Information Technology, Chinese Academy of Sciences, Shanghai 200050, China.*

[c] *Key Laboratory of Artificial Structures and Quantum Control (MOE), School of Physics and Astronomy, Shanghai Jiao Tong University, 800 Dongchuan Road, Shanghai 200240, China.*

[d] *State Key Laboratory of ASIC and System, Fudan University, Shanghai 200433, China*

[e] *Collaborative Innovation Center of Extreme Optics, Shanxi University, Taiyuan, Shanxi 030006, China.*

*Correspong author Email: xwu@ee.ecnu.edu.cn

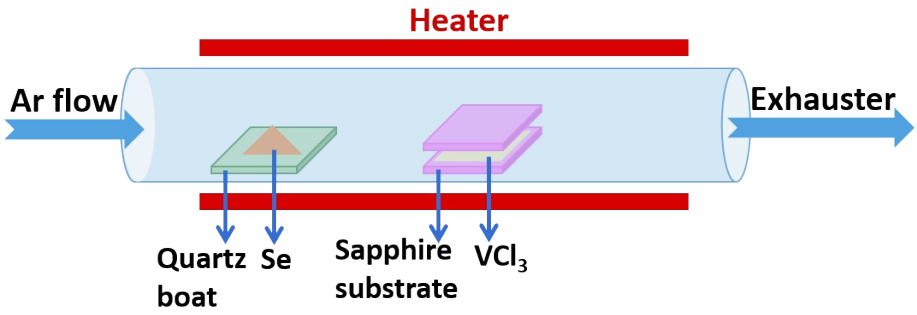

Figure S1 Schematic illustration of the growth route of VSe_2 nanosheets by CVD.

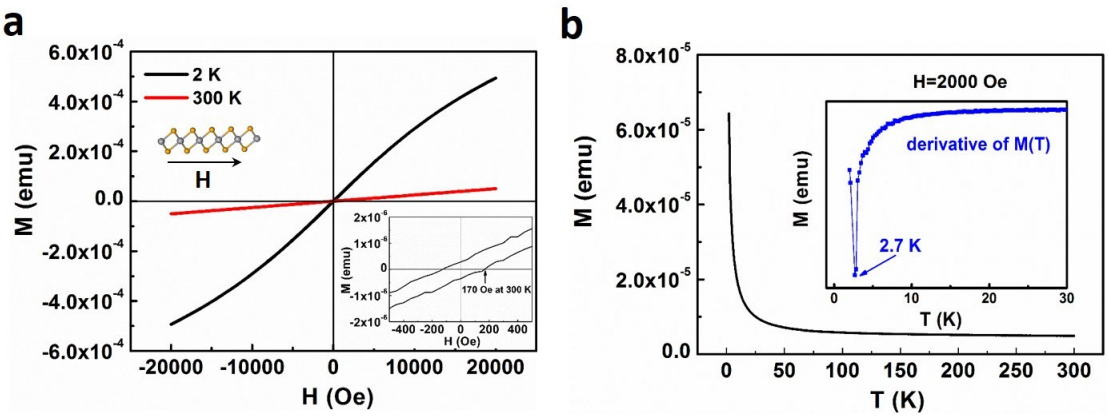

Figure S2 Magnetism characterization of VSe_2 nanosheets. (a) Magnetization versus magneitc field curves of VSe_2 at 2 K and 300 K. The inset is the coercivity of VSe_2, about 170 Oe at 300 K. Both of the coercivities at 2 K and 300 K are small. The magnetic field is parallel to the (001) plane of VSe_2. The weigth of the VSe_2 is 1 mg. (b) magnetization versus temperature curve of VSe_2 from 2 K and 300 K measured on the condition of zero-magneic-field cooling (ZFC) under magnetic field of 2000 Oe. From the curve, the VSe_2 behaves like ferromagnetic. The inset is the derivative of the ZFC magnetization curve, which shows a critical point at 2.7 K.

The magnetic hysteresis loops of VSe_2 nanosheets measured at 2 K and 300 K are shown in Figure S2a. The contribution from the substrate has been removed by measuring a blank substrate without sample. At 2 K, the hystersis loop presents a weak ferromagnetic-like curve with a small coercivity ~50 Oe. While the M-H curve of VSe_2 nanosheets presents a straight line at 300 K, showing a paramagnetic behavior, which conforms to the Curie's law:

$$C/T = M/H \qquad (1)$$

where C is the Curie constant. The coercivity of the hysteresis loop at 300 K is ~170 Oe. The larger coercivity of VSe_2 at 300 K shown in the inset of Figure S2a may be due to the small slope of M-H curve. Figure S2b is the M-T curve of the VSe_2 nanosheets from 2 K to 300 K under the magnetic field of 2000 Oe. The absence of saturation of the M-T curve with the decrease of temperature indicates the paramagnetic nature of the sample consisting with the M-

H curves. This is also demonstrated by the monotonic decreasing of the first-order derivation of the M-T curve, except the first two data points shown in the inset of Figure S2b.

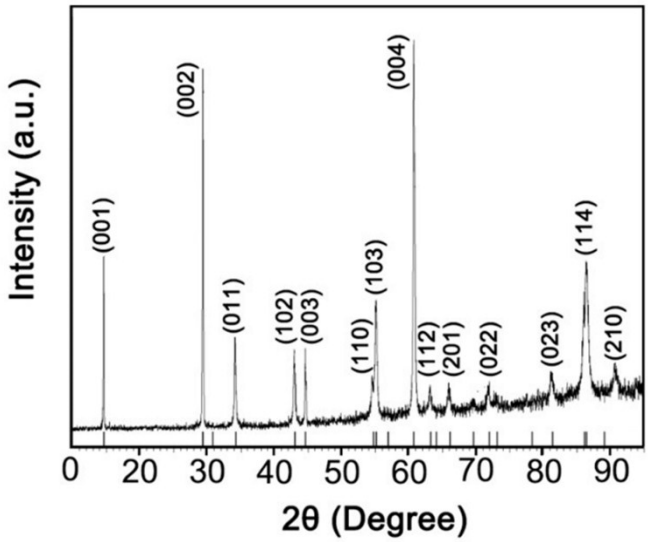

Figure S3 The X-ray diffraction (XRD) pattern of 1T-VSe_2 powder. The XRD pattern is in accordance with the standard JCPDS card No. 89-1641 of 1T-VSe_2. The diffraction peaks are indexed by the crystal plane. The sharp diffraction peaks and no impurity peaks demonstrate the high quality of the prepared VSe_2 nanosheets. The short bars below the diffraction pattern are the calculated positions of Bragg peaks of the 1T-VSe_2.

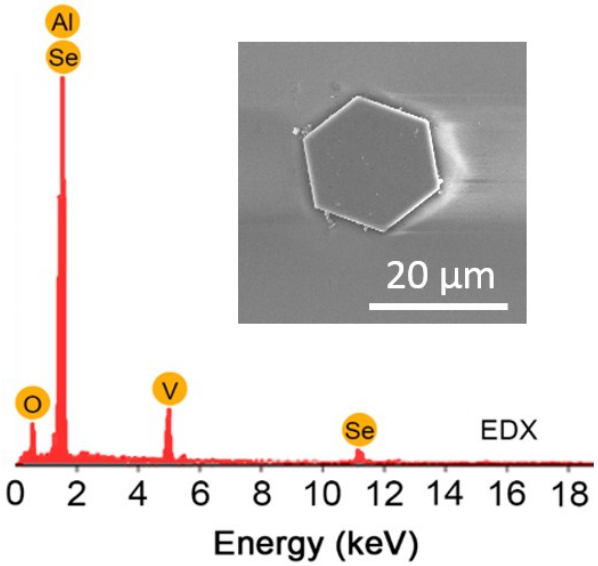

Figure S4 The SEM image and corresponding EDX spectrum of the VSe_2 nanosheet. The element ratio of V : Se is 2.2 close to the stoichiometry of VSe_2. The peaks of the spectrum are indexed by O, Al elements from the substrate and V, Se elements from the sample. The inset shows a secondary electron image of hexagonal VSe_2 samples with the size around 20 μm.

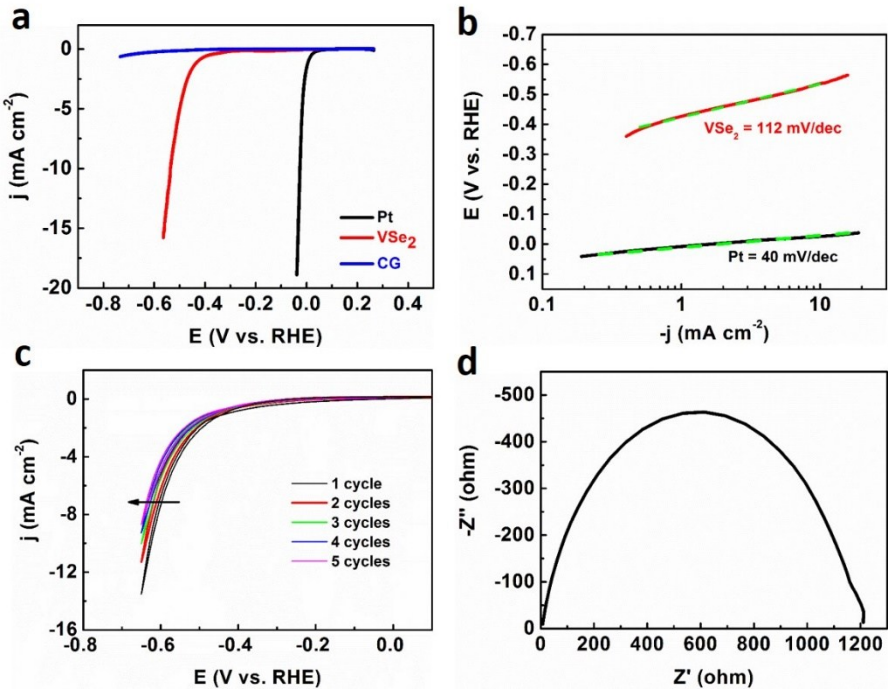

Figure S5 Electrocatalytic performance of VSe_2 nanosheets. (a) Polarization curves of Pt, VSe_2, and carbon glass (CG). (b) Corresponding Tafel plot of Pt and VSe_2. (c) Polarization curves of VSe_2 for 5 cycles. (d) Nyquist plots of VSe_2 nanosheet. The prepared 1T-VSe_2 single crystal nanosheets were also tested for the electrocatalytic hydrogen evolution reaction (HER). VSe_2 nanosheets was deposited on the carbon galss (CG) electrode, and measured in 0.5 M H_2SO_4 using a standard three-electrode setup. A Pt electrode, the best material for HER was tested for comparison. Figure S5a is the polarization curves of Pt, VSe_2 and CG electrode measured at the scan rate of 5 mV/s. Clearly, Pt has the best performance, lower than -0.05 V overpotential at -10 mA/cm^2, while the overpotential of VSe_2 nanosheets are larger than -0.5 V at -10 mA/cm^2. The CG does not show obvious catalytic effect even at -0.8 V. The corresponding Tafel plots fitted at small over potential region are shown in Figure S5b. The slopes of VSe_2 and Pt Tafel plots fitted by straight lines are 112 mV/dec and 40 mV/dec, respectively. During the durability test of VSe_2 for HER, the over potential graduatly increases, and the current graduatly decreases. The electrochemical impedance spectroscopy (EIS) test at a small over potential presents a charge transfer resistance of 1200 Ω.

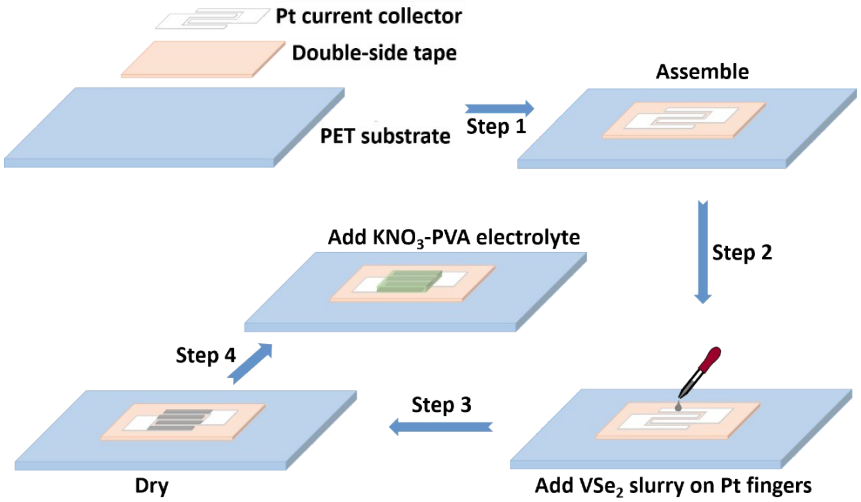

Figure S6 Flow chart of the fabrication of flexible in-plane solid-state VSe_2 supercapacitor.

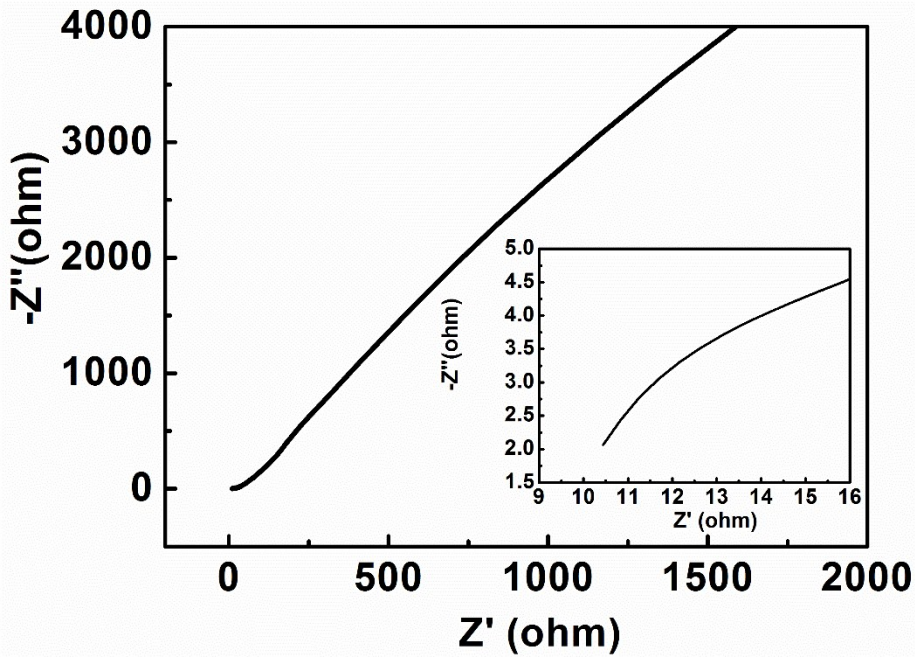

Figure S7 Impedance of the VSe_2 supercapacitor. The amplification of the beginning of the impedance curve is shown in the inset. The starting resistance, ~10.5 Ω, as shown in the inset demonstrates a small resistance of the supercapacitor that includes electrolyte resistance, Pt current-collector resistance, VSe_2 electrode-decoration-material resistance, and the contact resistance between the Pt and VSe_2 electrode decoration. There is no obvious semicircle in the impedance curve, even in the enlarged region of the beginning of the measurement as shown in the inset. It means that the charge and discharge processes of the supercapacitor are mainly controlled by the mass transfer process, and the charge transfer resistance is small.

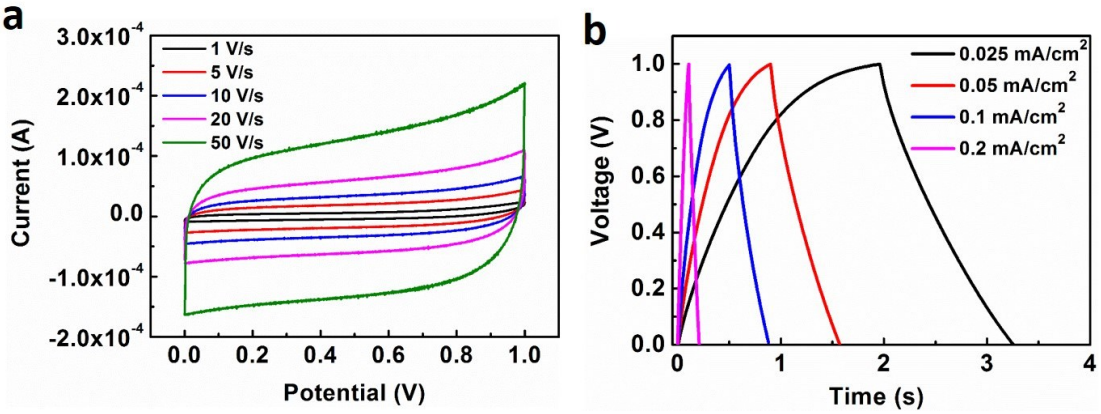

Figure S8 Electrchemical measurement of the in-plane Pt supercapcactior. (a) Cyclic voltammetry curves for the in-plane Pt supercapacitor at 1–50 V s^{-1}. The rectangular curves indicate the EDLC behavior. (b) Galvanostatic charge-discharge curves at the specific current density of 0.025–0.2 mA/cm^2. The quasi-trianglar shapes further confirm the EDLC behavior. The in-plane Pt supercapacitor without the decoration of VSe_2 nanosheets show a small capacitance. The highest capacitance calculated from the CD curves is 39 μF/cm^2 at 0.1 mA/cm^2, more than two orders smaller than that of the VSe_2 decorated in-plane supercapcitor.

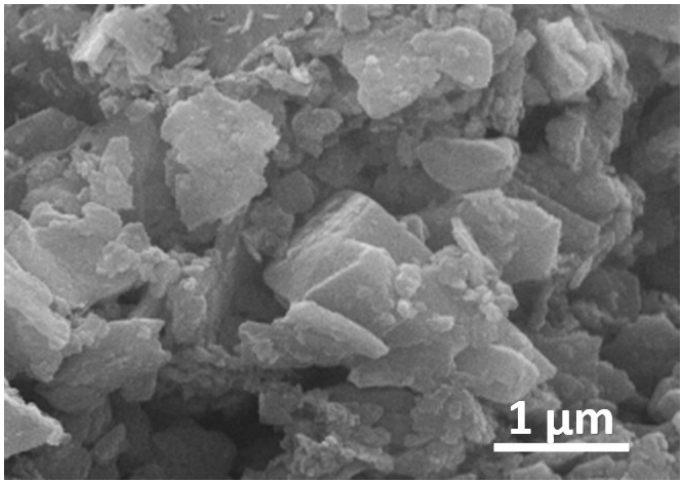

Figure S9 SEM characterization of the VSe_2 supercapacitor. The surface structure of the supercapacitor is composed of layered VSe_2 nanosheets and vacancies, which provides large specific surface and channels for reversable K^+ adsorption and penetration

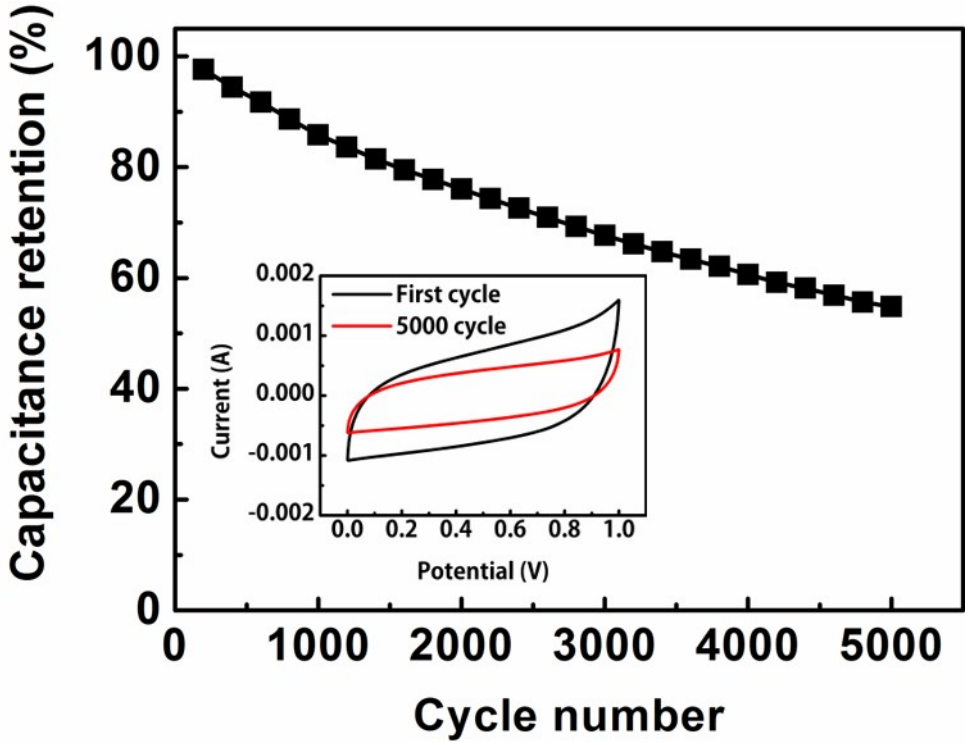

Figure S10 Cycling stability of the VSe_2 in-plane supercapacitor after 5000 cycles, 55% capacity is retained.

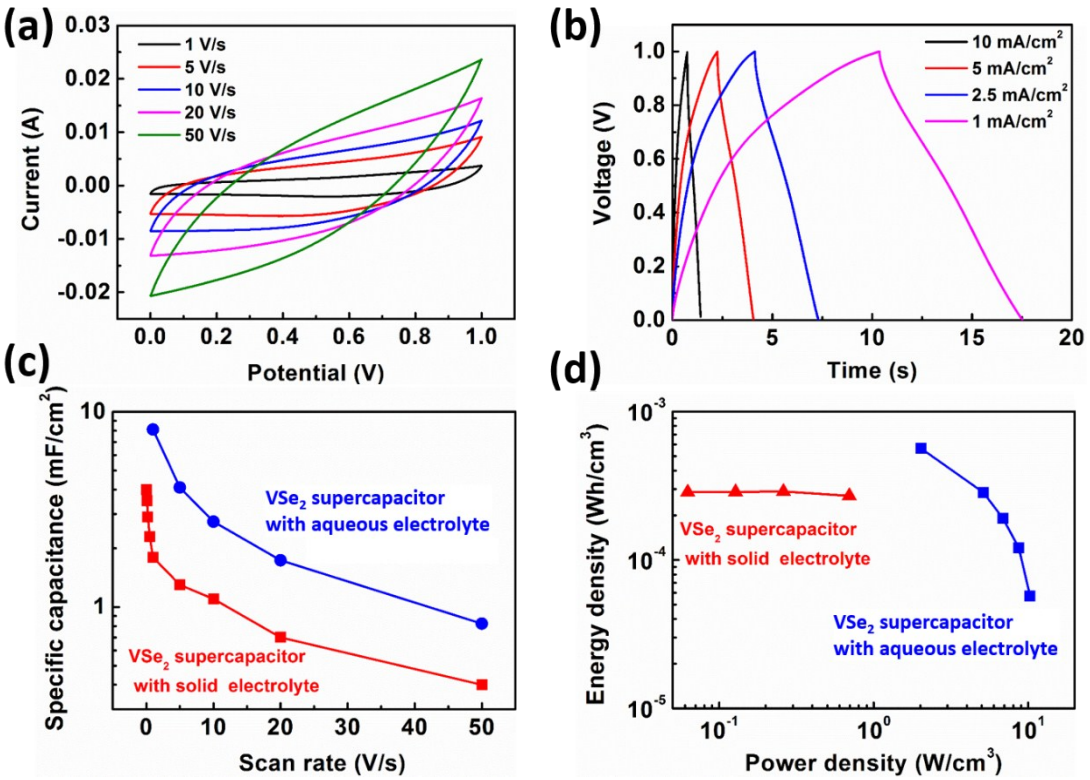

Figure S11 Performance of VSe_2 supercapacitor with aqueous electrolyte (1 M KNO3 solution) and the comparison with that of the solid electrolyte (PVA/KNO_3). (a) Cyclic voltammetry curves of the aqueous-electrolyte in-plane supercapacitor of VSe_2 at 1-50 V s^{-1}. (b) Galvanostatic charge-discharge curves of the solid-electrolyte in-plane supercapacitor of VSe_2 at the specific current density of 1-10 mA/cm^2. The quasi-triangular shapes demonstrate the EDLC behavior that is consist with the cyclic voltammetry results. (c) Specific capacitance of in-plane VSe_2 supercapacitors with solid and aqueous electrolyte. (d) Ragone plot of in-plane VSe_2 supercapacitors with solid and aqueous electrolyte.

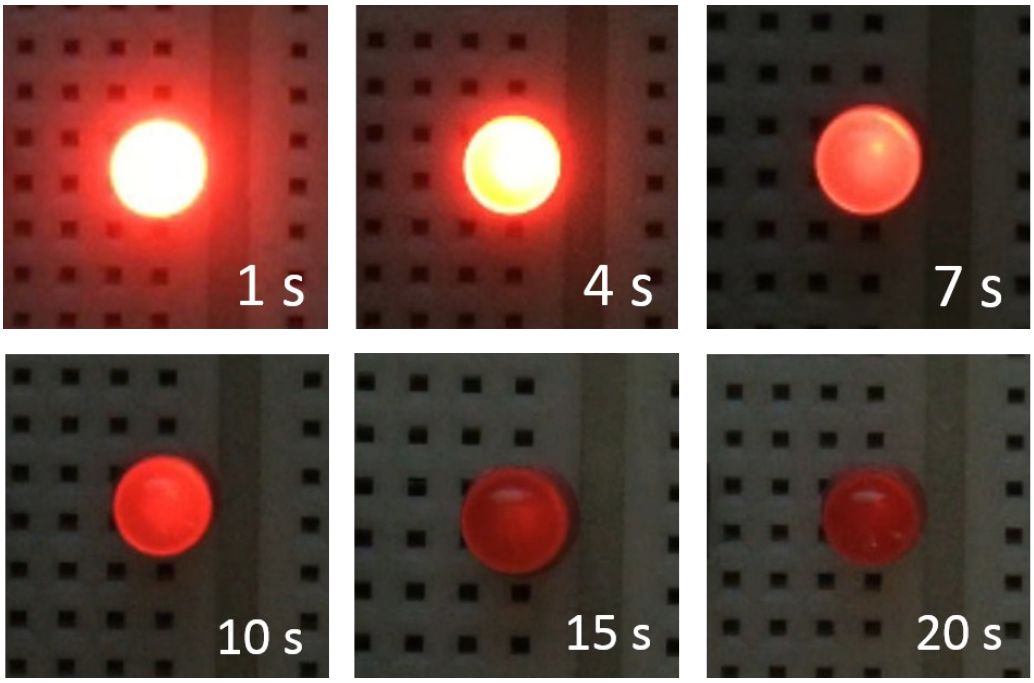

Figure S12 Demonstration of a LED light powered by the in-plane supercapacitor.

References:

[1] J. Feng, X. Sun, C. Wu, L. Peng, C. Lin, S. Hu, J. Yang, Y. Xie, Metallic few-layered VS_2 ultrathin nanosheets: high two-dimensional conductivity for in-plane supercapacitors, J. Am. Chem. Soc. 133, (2011) 17832-17838.

[2] Y. Z. Yu, J. Zhang, X. Wu, Z. Q. Zhu, Facile ion-exchange synthesis of silver films as flexible current collectors for micro-supercapacitors, J. Mater. Chem. 3, (2015) 21009-21015.

Supplementary Movie 1: LED lighting powered by the supercapacitor.

Supplementary Movies 2: Bending test.